Monitoring the Daily Rhythm of Total Green Leaf Volatiles with a Low-Cost Multi-Sensor Node

Filipe Cardoso
Centro de Informática
Universidade Federal de Pernambuco
Recife, Brazil
fmlcc@cin.ufpe.br

Stefan Blawid
Centro de Informática
Universidade Federal de Pernambuco
Recife, Brazil
ORCID 0000-0001-6982-4575

2022 Symposium on Internet of Things (SIoT) | 978-1-6654-7475-7/22/$31.00 ©2022 IEEE | DOI: 10.1109/SIOT56383.2022.10069883

***Abstract*—Plants emit volatile organic compounds (VOCs) from their leaves, flowers or fruits. These chemical signals have many functions ranging from hormonal regulation to complex interactions with pollinators and herbivores. Even diseases can influence the emission of VOCs. Thus, VOC monitoring might allow to deduce the abiotic and biotic stress of plants and to support data based decisions on countermeasures. However, most sensing methods for VOCs are not low-cost and mobile, which hinders widespread application. We report here on the possibility of employing off-the-shelf air quality sensors for sensing VOC levels emitted by plants. The developed low-cost multi-sensor node is described in detail. As a proof of principle, we monitor the VOC emission from the subshrub rue and show that a cyclic day-night rhythm of total VOC emission can be observed.**

***Index Terms*—Volatile organic compounds, Precision agriculture, IoT, Low-cost sensor, Digital decision systems**

I. Introduction

Digital decision support systems (DSS) based on crop, soil and weather data can assist small scale farmers in correctly choosing the timing and intensity of applying pesticides, fertilizers or irrigation [1]. Smallholder farming constitutes an important segment of the Brazilian agriculture. More than 70% of the country's agricultural cooperatives are based on family farms and smallholder farming contributes 23% to the total Brazilian agricultural production [2]. Moreover, small scale growers play an important role in maintaining the genetic diversity of crops. Despite this importance, smallholder farmers receive only limited technical advise to manage efficiently the available scarce resources for maximizing the harvest and avoiding crop losses. In addition, the traditional generational knowledge transfer is threatened by an aging rural population, rural exodus, and shifting growing conditions due to climate change. Thus, DSSs could become an essential enabling technology for informed cultivation decisions in smallholder farming.

Measurable properties for crop monitoring include height, color, and the presence of pests and diseases. Thus, most studies beyond the laboratory scale report on the use of optical sensors [3]–[5]. A less obvious but rather interesting measurement parameter are volatile organic compounds (VOCs) emitted by the plant. Ethylene, e.g., is a gaseous ripening phytohormone of fruits and plants and its monitoring helps to control the ambient conditions throughout transport and the whole supply chain [6]. Most sensing methods for VOCs, like photoionization, spectroscopy, chromatography and e-noses, are not mobile *and* low cost [7]–[9]. A notable exception are amperometric and resistive sensors. A widely used example of the latter are tin oxide sensors, which are based on the reaction of the analyte gas with adsorbed oxygen on the metal oxide surface leading to a change in the electron density of $\mathrm{SnO_2}$. Although metal oxide sensors have many disadvantages, like unspecified signal-to-noise ratio, slow response times, changing baseline and non specific gas detection, they were recently employed to monitor light and water stress of plants, e.g., during transport, signaled by the total VOC emission [10].

We report here on a low-cost sensor node to be used in DSSs that integrates two off-the-shelf indoor air quality modules based on resistive gas sensing. As a proof of principle we monitor the total VOC emission of a common herb during the day-night cycle.

II. Significance of Volatile Organic Compounds

Potential application of VOC sensing goes well beyond the control of ambient conditions during transport of fruits and plants. First, it is well known that plants use VOCs as chemical defense against herbivores by directly affecting the attacker (or its microbiome) and/or by attracting predators [11]–[13]. Moreover, disease agents like viruses can also modify the VOC emission to call for mobile vectors for their spreading. In both cases, threat detection (and the decision to apply pesticides) might be based on VOC sensing. Finally, abiotic stress, like elevated $\mathrm{CO_2}$ levels and drought, leads also to changes in the VOC profile (probably due to an altered microbiome), which could be monitored.

To test the sensitivity of the developed sensor node, we turn to a simpler interaction system. The plant metabolism changes with the available light [14]. Daily changes can be also expected for the VOC emission. Many herbs are fragrant. Like floral volatiles, the responsible VOCs might be emitted rhythmically following the activity patterns of pollinators or herbivores during the day-night cycle [15]. Indeed, plants exhibit an endogenous circadian clock that controls the rhythmic emission even in the absence of light cues.

This work was supported by the Conselho Nacional de Desenvolvimento Científico e Tecnológico under a Productivity Grant.

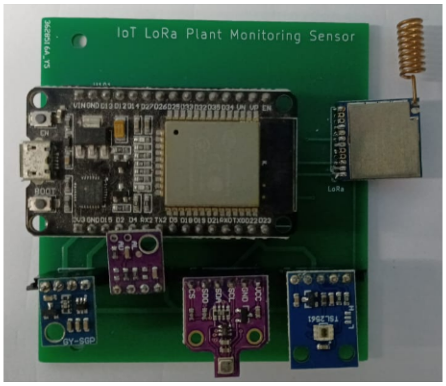

Fig. 1. IoT LoRa/WiFi Plant Monitoring sensor.

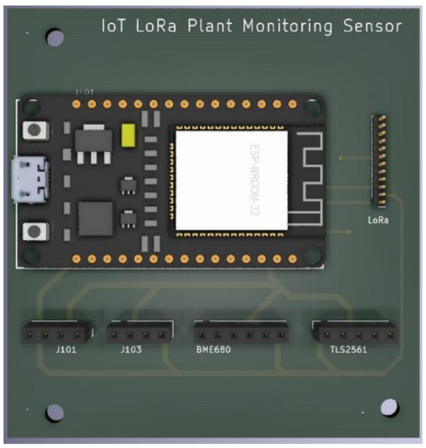

Fig. 2. Design of the printed circuit board.

We measured the daily changes of the total VOC emission of the ornamental plant and herb rue (*Ruta graveolens*) that is known for its aromatic leaves and insect repellent effect.

III. Low-Cost Multi-Sensor Node

The assembled low-cost multi-sensor node for LoRa/WiFi networks is shown in Fig. 1. The printed circuit board, Fig. 2, was designed with KiCad, an open source electronics design automation suite [16]. The board hosts four sensors: Sensirion's SGP30 outputs total volatile organic compounds, tVOCs [ppb], and is complemented by the SHT31 that outputs temperature, T [$^\circ$C], and relative humidity, RH [%]; the Bosch BME680 converts its sensor inputs into an air quality index, IAQ [a number]; and ams OSRAM's TSL2561 measures illuminance, E_{V} [lux]. The sensors, Fig. 3, were selected based on the results and discussions presented in [10].

In general, air quality sensors do not output raw data. The tVOC values given by the SGP30 are the result of internal conversion and baseline compensation algorithms. Additional on-chip humidity compensation is applied when the data of the SHT31 are sent to the SGP30 unit. The BME680 even integrates the signal of the metal-oxide sensor with temperature, humidity and pressure measurements to an overall air quality index. Thus, these air quality sensors are only suitable for

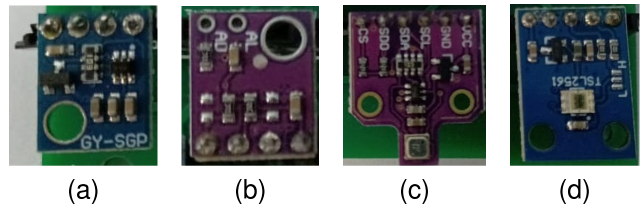

Fig. 3. (a) SGP30 - Indoor Air Quality Sensor for TVOC and CO2eq Measurements [17], (b) SHT31 - Humidity and Temperature Sensor [18], (c) BME680 - Low power gas, pressure, temperature & humidity sensor [19], (d) TSL2561 - Light-to-digital converter [20].

monitoring VOC emission but not for absolute measurements. For the SGP30, the output values of ethanol/H_2 levels (raw data) range from $0\,\mathrm{ppm}$ to $1000\,\mathrm{ppm}$ and of tVOC (converted data) from $0\,\mathrm{ppb}$ to $60\,000\,\mathrm{ppb}$ [17].

The objective to include a temperature and humidity sensor into the node is twofold. First, the output can be used to compensate the baseline of the tVOC metal-oxide sensor for humidity effects. Second, the tVOC emission of the plant may be sensitive to ambient T and RH conditions. The standard return signal of the BME680, ranging from $\mathrm{IAQ} = 0$ (excellent air quality) to 500 (extremely polluted air), is not very useful for tVOC measurements. Nevertheless, changes in tVOC emission might be reflected in changes of IAQ that might help to verify the tVOC signal from the SGP30. Moreover, access to the raw data for pressure, temperature, relative humidity, and gas sensor resistivity, as well as to converted data like sensor compensated resistivity or breath VOC equivalents is possible although not attempted in the present work. Finally, the illuminance data from the TSL2561 are essential to correlate the tVOC signal to light cues.

All sensors are connected via an I^2C bus to a $2.4\,\mathrm{GHz}$ WiFi and Bluetooth MCU module, an ESP32-WROOM-32 from Espressif [21], that includes a dual core 32-bit microprocessor. In the current development state of the sensor node the ESP32 provides a broad range of connectivity options to read out the sensor signals and serves as a generic IoT sensor hub. The sensor node also hosts a LoRA RA-01 module from IA-Thinker [22] that integrates Semtech's SX1276 [23], a LoRa core long-range low-power transceiver. In a later usage scenario, the LoRa RF modulation (instead of frequency shift keying) and the provided $18\,\mathrm{dBm}$ output power and $2.5\,\mathrm{dBi}$ spring antenna should allow direct and wireless data transmission robust against interference between a smart greenhouse and a monitoring station. The specified energy consumption is low, typical supply currents amount to $1.6\,\mathrm{mA}$, $12\,\mathrm{mA}$ and $93\,\mathrm{mA}$ at $3.3\,\mathrm{V}$ supply voltage for idle, receive and transmission mode, respectively. We developed a web app employing Google's Firebase platform to log sampled data from the sensors to a real time database based on http requests. The required client libraries are installed on the ESP32.

Relevant software to reproduce the described low-cost multi-sensor node have been provided on Github: https://github.com/FilipeMesel/mestrado.

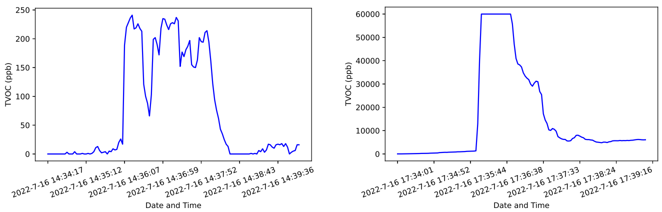

(a) (b)

Fig. 4. Sampled tVOC data when the multi-sensor node is exposed to (a) human breathing and (b) scent. Note the different scale in (a) and (b).

IV. Functional Tests

To verify the ability of the SGP30 sensor to capture significant differences in the particle density of VOCs present in the environment, we carried out a couple of functional tests. In the first test, human breath was monitored. During a period of five minutes, a test person breathed in the vicinity of the sensor. The results are shown in Fig. 4(a). As soon as the test person started to breath close to the sensor the tVOC level raised from nearly zero up to $250\,\mathrm{ppb}$. Even the rhythm of in- and out breathing could be monitored. As soon as the test person went away from the sensor, the tVOC levels dropped again to nearly zero. As expected for an indoor tVOC sensor, the SGP30 is sensitive enough to perceive aspects of human breathing. The test also confirmed that sensor data could be successfully transmitted to the Firebase real time database. A Python script was employed to visualize the sampled data.

The second test aimed to reach the maximum concentration of VOCs detectable by the sensor. A sheet of scented paper was waved on top of the SGP30 for a period of two minutes. The data acquired from such an experiment are shown in Fig. 4(b), detailing the period in which the sheet of paper was used. Indeed the presence of perfume in the environment is sufficient to saturate the SGP30 at its theoretical limit of $60\,000\,\mathrm{ppb}$.

V. Results

The main experiment carried out in the present work aimed to investigate the sensor's ability to detect the presence and temporal patterns of tVOCs emitted by rue (*Ruta graveolens*) samples. Rue is a subshrub with dense foliage that has a characteristic odor, alternate leaves and small flowers. This plant was chosen because it is not demanding in terms of climate and forms of cultivation, because it has a characteristic odor, because it is easily accessible in the region where the research was carried out and because it is used for medicinal purposes as a treatment against inflammation in the eyes.

Two specimens of the aforementioned rue were planted in a jar and the sensor was mounted on a wooden support capable of holding the whole circuit board on top of the plants. The experiment was conducted in an open area that allowed the contact of the plant with the external environment, see Fig. 5. The tVOC emission together with other environmental data were sampled over a period of two days and two nights and

Fig. 5. The sensor was placed above the investigated rue by a wooden support.

repeated after a break of a couple of days. The sampled data are shown in Fig. 6. To suppress noise we averaged the sensor data obtained in the period from 5am to 5pm (day) and from 5pm to 5am (night). The mean values of each data set (tVOC, humidity, temperature, pressure, illuminance) were normalized to its value obtained for the second day.

As expected, the illuminance (rightmost bar in Fig. 6) oscillates between day and night. During the night period the normalized illuminance drops to a very low value and the corresponding bar in the chart is not visible during the night periods. Most importantly, other environmental factors that could influence the tVOC emission of the plant, like humidity, temperature and pressure, remained fairly constant during the day-night cycle. The environmental data are typical for a tropical climate, e.g., sudden sunsets (sunrises) and low temperature variation.

However, in both repetitions of the experiment we found a clearly perceivable cyclic pattern of the tVOC emission. During the day rue emits on average a larger amount of tVOCs than during the night. This day-night cycle is highlighted by the bold line in Fig. 6(b). Since most of the environmental data are stable, we conclude that this periodic pattern reflects metabolic changes of rue only triggered by light cues. Finally, we observed in addition an overall rise in the tVOC levels during the monitoring period in the first experiment, see Fig. 6(a). Only additional experiments can elucidate if the observed behavior indeed reflects an accumulation of tVOCs in the plant headspace or is caused by a shift in the sensor baseline.

VI. Conclusion

Sensing the variations of volatile organic compounds emitted from plants could be an indicator of biotic or abiotic stress and thus be useful in precision agriculture. Today, the main techniques of assessing the concentration of VOCs still require laboratory procedures. The results presented here hint to the possibility of integrating off-the-shelf electronic air quality sensors for the purpose of VOC sensing in agriculture. Low-cost and mobile electronic systems would allow real-

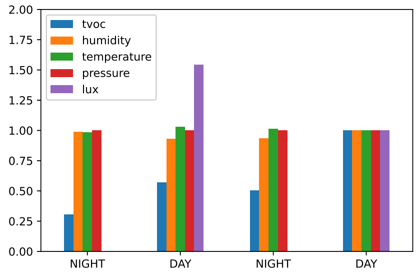

(a)

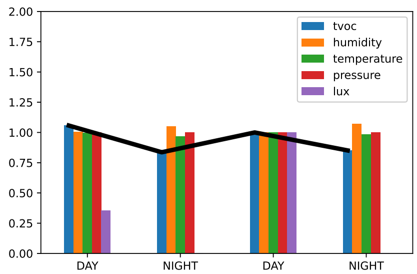

(b)

Fig. 6. Mean values of sampled sensor data during two monitoring periods (a,b) of two days each. The mean values are normalized to the value of the second day, e.g., tVOC=995 ppb, RH=62 %, T=32 °C, p=101.4 Pa, E_{V}=3001 lx in (b). In both periods the tVOC concentration followed a day-night cycle, highlighted by a bold line for the second period (b). In the first monitoring period (a) also an overall increase of the tVOC levels was observed. In the absence of the subshrub rue the ambient level of tVOCs amounts to ca. 180 ppb (ca. 0.18 after normalization).

time monitoring and could be deployed in crop fields, gardens and greenhouses. As a result, a greater and more detailed data sampling is enabled. Such data could be used in digital decision support systems guiding agricultural activities. We demonstrated the sensitivity of such air quality sensors by revealing the cyclic production and emission of total VOCs from the subshrub rue.

However, the use of commercially available air quality sensors is challenging. The sensing principle is not discriminatory to the specific VOCs emitted by plants. Only total VOC concentrations can be monitored. Moreover, many air quality sensors obscure the access to the raw gas sensor resistivity and output equivalent measures instead. The measurement principles of metal-oxide sensors is also susceptible to failures and baseline shifts. In our experiments we repeatedly observed time periods with a malfunctioning sensor. The complexity of VOC signals will also call for machine learning algorithms and artificial intelligence for interpreting the sampled data.

References

[1] A. P. Antony, K. Leith, C. Jolley, J. Lu, and D. J. Sweeney, "A Review of Practice and Implementation of the Internet of Things (IoT) for Smallholder Agriculture," *Sustainability*, vol. 12, no. 9, p. 3750, 2020.

[2] IBGE, *Agricultural Census 2017*, accessed July 13, 2022. [Online]. Available: https://censoagro2017.ibge.gov.br/templates/censo_agro/resultadosagro/index.html

[3] M. Friedli, N. Kirchgessner, C. Grieder, F. Liebisch, M. Mannale, and A. Walter, "Terrestrial 3D laser scanning to track the increase in canopy height of both monocot and dicot crop species under field conditions," *Plant Methods*, vol. 12, no. 1, p. 9, 2016.

[4] E. Mwebaze and G. Owomugisha, "Machine Learning for Plant Disease Incidence and Severity Measurements from Leaf Images," in *15th IEEE International Conference on Machine Learning and Applications (ICMLA)*, 11 2016, pp. 158 – 163.

[5] M. d. S. Barros, I. d. M. Philippini, L. G. Silva, A. B. d. S. Netto, R. Blawid, E. N. d. S. Barros, and S. Blawid, "Supervised Training of a Simple Digital Assistant for a Free Crop Clinic," in *10th Brazilian Conference on Intelligent Systems, BRACIS*, 11 2021, pp. 162–176.

[6] S. Janssen, K. Schmitt, M. Blanke, M. L. Bauersfeld, J. Wllenstein, and W. Lang, "Ethylene detection in fruit supply chains," *Philosophical Transactions of the Royal Society A: Mathematical, Physical and Engineering Sciences*, vol. 372, no. 2017, p. 20130311, 2014.

[7] U. Garlando, L. Bar-On, A. Avni, Y. Shacham-Diamand, and D. Demarchi, "Plants and Environmental Sensors for Smart Agriculture, an Overview," in *IEEE Sensors*, 10 2020, pp. 1–4.

[8] L. Spinelle, M. Gerboles, G. Kok, S. Persijn, and T. Sauerwald, "Review of Portable and Low-Cost Sensors for the Ambient Air Monitoring of Benzene and Other Volatile Organic Compounds," *Sensors*, vol. 17, no. 7, p. 1520, 2017.

[9] D. Tholl, W. Boland, A. Hansel, F. Loreto, U. S. R. Röse, and J. P. Schnitzler, "Practical approaches to plant volatile analysis," *Plant Journal*, vol. 45, no. 4, pp. 540 – 560, 02 2006.

[10] A. Catini, L. Papale, R. Capuano, V. Pasqualetti, D. D. Giuseppe, S. Brizzolara, P. Tonutti, and C. D. Natale, "Development of a sensor node for remote monitoring of plants," *Sensors*, vol. 19, no. 22, p. 4865, 11 2019.

[11] H. Bouwmeester, R. C. Schuurink, P. M. Bleeker, and F. Schiestl, "The role of volatiles in plant communication," *Plant Journal*, vol. 100, no. 5, pp. 892 – 907, 12 2019.

[12] J. J. Beck, H. T. Alborn, A. K. Block, S. A. Christensen, C. T. Hunter, C. C. Rering, I. Seidl-Adams, C. J. Stuhl, B. Torto, and J. H. Tumlinson, "Interactions among Plants, Insects, and Microbes: Elucidation of Inter-Organismal Chemical Communications in Agricultural Ecology," *Journal of Agricultural and Food Chemistry*, vol. 66, no. 26, pp. 6663 – 6674, 07 2018.

[13] M. Heil and R. Karban, "Explaining evolution of plant communication by airborne signals," *Trends in Ecology and Evolution*, vol. 25, no. 3, pp. 137 – 144, 03 2010.

[14] D. J. Liebelt, J. T. Jordan, and C. J. Doherty, "Only a matter of time: the impact of daily and seasonal rhythms on phytochemicals," *Phytochemistry Reviews*, vol. 18, no. 6, pp. 1409–1433, 2019.

[15] L. Zeng, X. Wang, M. Kang, F. Dong, and Z. Yang, "Regulation of the Rhythmic Emission of Plant Volatiles by the Circadian Clock," *International Journal of Molecular Sciences*, vol. 18, no. 11, p. 2408, 2017.

[16] KiCad-Project, *KiCad EDA*, accessed July 11, 2022. [Online]. Available: https://www.kicad.org

[17] Sensirion, *Datasheet of SGP30 - Indoor Air Quality Sensor for TVOC and CO2eq Measurements*, accessed July 15, 2022. [Online]. Available: https://sensirion.com/media/documents/984E0DD5/61644B8B/Sensirion_Gas_Sensors_Datasheet_SGP30.pdf

[18] ——, *Datasheet of SHT3x-DIS - Humidity and Temperature Sensor*, accessed July 11, 2022. [Online]. Available: https://sensirion.com/media/documents/213E6A3B/61641DC3/Sensirion_Humidity_Sensors_SHT3x_Datasheet_digital.pdf

[19] Bosch, *Datasheet of BME680 - Low power gas, pressure, temperature & humidity sensor*, accessed July 11, 2022. [Online]. Available: https://www.bosch-sensortec.com/media/boschsensortec/downloads/datasheets/bst-bme680-ds001.pdf

[20] ams OSRAM, *Datasheet of TSL2561 - Light-to-digital converter*, accessed July 11, 2022. [Online]. Available: https://ams.com/documents/20143/36005/TSL2561_DS000110_3-00.pdf/18a41097-2035-4333-c70e-bfa544c0a98b

[21] Espressif, *Datasheet of ESP32-WROOM-DA*, accessed July 21, 2022. [Online]. Available: https://www.espressif.com/sites/default/files/documentation/esp32-wroom-32_datasheet_en.pdf

[22] AI-Thinker, *Specification of Ra-01 LoRa Module*, accessed July 27, 2022. [Online]. Available: https://docs.ai-thinker.com/_media/lora/docs/c047ps01a1_ra-01_product_specification_v1.1.pdf

[23] SEMTECH, *Datasheet of SX1276*, accessed July 27, 2022. [Online]. Available: https://semtech.my.salesforce.com/sfc/p/#E0000000JelG/a/2R0000001Rbr/6EfVZUorrpoKFfvaF_Fkpgp5kzjiNyiAbqcpqh9qSjE